Journal of *Marine Science and Engineering*

MDPI

Article

Giant Submarine Landslide in the South China Sea: Evidence, Causes, and Implications

Chaoqi Zhu [1,2], Sheng Cheng [1], Qingping Li [3], Hongxian Shan [1,2,4], Jing'an Lu [5], Zhicong Shen [1], Xiaolei Liu [1,2,4] and Yonggang Jia [1,2,4,*]

1 Shandong Provincial Key Laboratory of Marine Environment and Geological Engineering, Ocean University of China, Qingdao 266100, China; george-zhu@foxmail.com (C.Z.); cs9554@stu.ouc.edu.cn (S.C.); hongxian@ouc.edu.cn (H.S.); shenzhicong@stu.ouc.edu.cn (Z.S.); xiaolei@ouc.edu.cn (X.L.)
2 Laboratory for Marine Geology, Qingdao National Laboratory for Marine Science and Technology, Qingdao 266061, China
3 Research Center of China National Offshore Oil Corporation, Beijing 100027, China; liqp@cnooc.com.cn
4 Key Lab of Marine Environment and Ecology, Ministry of Education, Qingdao 266100, China
5 Guangzhou Marine Geological Survey, China Geological Survey, Guangzhou 510075, China; luja@gmgs.cn
* Correspondence: yonggang@ouc.edu.cn

Received: 6 April 2019; Accepted: 13 May 2019; Published: 17 May 2019

Abstract: Submarine landslides can be tremendous in scale. They are one of the most important processes for global sediment fluxes and tsunami generation. However, studies of prodigious submarine landslides remain insufficient. In this review paper, we compile, summarize, and reanalyze the results of previous studies. Based on this reanalysis, we discover the giant Baiyun–Liwan submarine slide in the Pearl River Mouth Basin, South China Sea. We describe three concurrent pieces of evidence from ~23 Ma to 24 Ma, the Oligocene–Miocene boundary, for this landslide: the shoreward shift of the shelf break in the Baiyun Sag, the slump deposition to the southeast, and the abrupt decrease in the accumulation rate on the lower continental slope. This landslide extends for over 250 km, and the total affected area of the slide is up to ~35,000–40,000 km^2. The scale of the landslide is similar to that of the Storegga slide, which has long been considered to be the largest landslide on earth. We suggest that strike–slip movement along the Red River Fault and ridge jump of the South China Sea caused the coeval Baiyun–Liwan submarine slide. The identification of the giant landslide will promote the understanding of not only its associated geohazards but also the steep rise of the Himalayan orogeny and marine engineering. More attention needs to be paid to areas with repeated submarine landslides and offshore installations.

Keywords: giant submarine landslides; shelf break; South China Sea; Himalayan orogeny; repeated submarine landslides

1. Introduction

Terrestrial landslides are efficient agents for the transport of rock, sediment, and carbon [1]. Alarmingly, submarine landslides on continental slopes can be more tremendous in scale—up to three orders of magnitude larger than terrestrial landslides in terms of total volume [2–4]. The volume of a single prodigious submarine landslide can be hundreds of times larger than the annual sediment flux from all the world's rivers to the ocean. An example is the Storegga slide, with over 3000 km^3 of sediment—long considered to be the largest submarine slide on earth [5,6]. Recently, a similar giant submarine landslide caused by the reactivation of major intra-plate faults, the Halibut Slide, was found in the North Atlantic [7]. The latest large submarine landslide triggered by the 2011 Tohoku earthquake covered an area of ~27.7 km^2 [8]. Prodigious submarine landslides are rare, but can dramatically alter seafloor morphology and sedimentary structure, generate huge tsunamis, and damage offshore

infrastructures [3,9–11]. The Grand Banks landslide in 1929 broke 12 telegraph cables and generated a tsunami with runup of 13 m [12]. A submarine landslide with a volume of ~5 km^3 in Papua New Guinea generated a tsunami killing 2200 people in 1999 [13]. The 2011 Tohoku tsunami with runups of 20 m was also exemplified by the part contribution of a submarine landslide [14]. Exploring giant submarine landslides on a long time scale will provide clues for global change and tectonic events. Giant submarine landslides attract immense research interest on the global level due to their geological, ecological, societal, and economical significance.

Submarine landslides are widespread in the Pearl River Mouth Basin (PRMB, Figure 1, [15]), which is the main reservoir of oil, gas, and gas hydrate in the northern South China Sea. However, many submarine landslides have been buried or obscured. It is difficult to recognize and map them accurately. Apart from numerous small-scale submarine landslides, 142 mass transport complexes with an average area of over 7 km^2 can be found in the submarine canyons of PRMB. In deeper waters, a series of Quaternary mass transport complexes with a total areal extent of ~11,000 km^2 and a conservative volume estimate of ~1035 km^3 are recognized [16,17]. Alarmingly, two large submarine landslides or submarine creep zones have been discovered in the PRMB, including the Baiyun slide (>13,000 km^2; ~0.3 Ma; Figure 1) and the Dongsha creep zone (>800 km^2; active at present; Figure 1) [18–20]. Here, we summarize several pieces of evidence and report the world's potentially largest landslide (the Baiyun–Liwan submarine slide, Figure 1) in the South China Sea, as well as its scale, timing, and triggering mechanism. It is proposed that the recognition and study of the giant Baiyun–Liwan submarine slide will promote the understanding of not only its associated geohazards but also the spreading of the South China Sea, the steep rise of the Himalayan orogeny, and marine engineering.

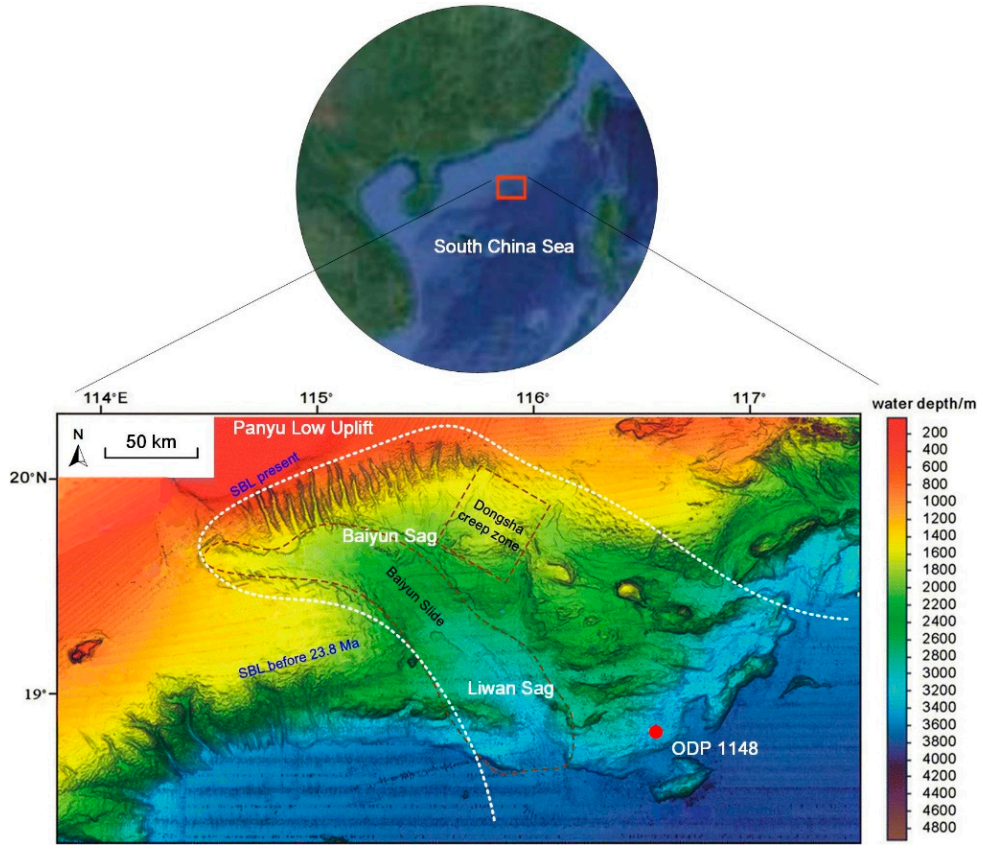

Figure 1. Multi-beam submarine geomorphology shadow map showing the Baiyun–Liwan submarine slide, the Baiyun slide, the Dongsha creep zone, and the shelf break line (SBL). The white dotted line is a scarp of the Baiyun–Liwan submarine slide. The brown dotted lines are the scarp of the Baiyun slide and range of the Dongsha creep zone, respectively.

2. Geological Setting

The Baiyun–Liwan submarine slide is located mainly at the Baiyun Sag and Liwan Sag, in the southern part of the PRMB and close to the continent–ocean boundary of the South China Sea [15]. The PRMB is the largest basin in the northern continental margin of the South China Sea. From north to south, the PRMB includes three uplifts and two depressions: the Northern Terrace, the Northern Depression (Zhu I Depression and Zhu III Depression), the Central Uplift (Shenhu Uplift, Panyu Low Uplift, and Dongsha Uplift), the Southern Depression (Zhu II Depression, and Chaoshan Depression), and the Southern Uplift (Figure 1) [21]. From bottom to top, eight formations are identified in the PRMB, namely, the Shenhu, Wenchang, Enping, Zhuhai, Zhujiang, Hanjiang, Yuehai, and Wanshan Formations. The PRMB experienced three major tectonic evolution stages: rifting (65–30 Ma), transition (30–23.8 Ma), and thermal subsidence (23.8 Ma–present) [15,22].

The Baiyun Sag is bordered by the Panyu Low Uplift to the north and the Liwan Sag and the Southern Uplift to the south (Figures 1 and 2). Covering an area of more than ~30,000 km^2 and exceeding 11 km in thickness, the Baiyun Sag and the neighboring Liwan Sag are the largest and deepest sags in the PRMB [23,24]. In addition, Liwan 3-1, the largest offshore platform in Asia, is built in the Baiyun Sag. Gas hydrate production tests were also conducted there in 2017 [25].

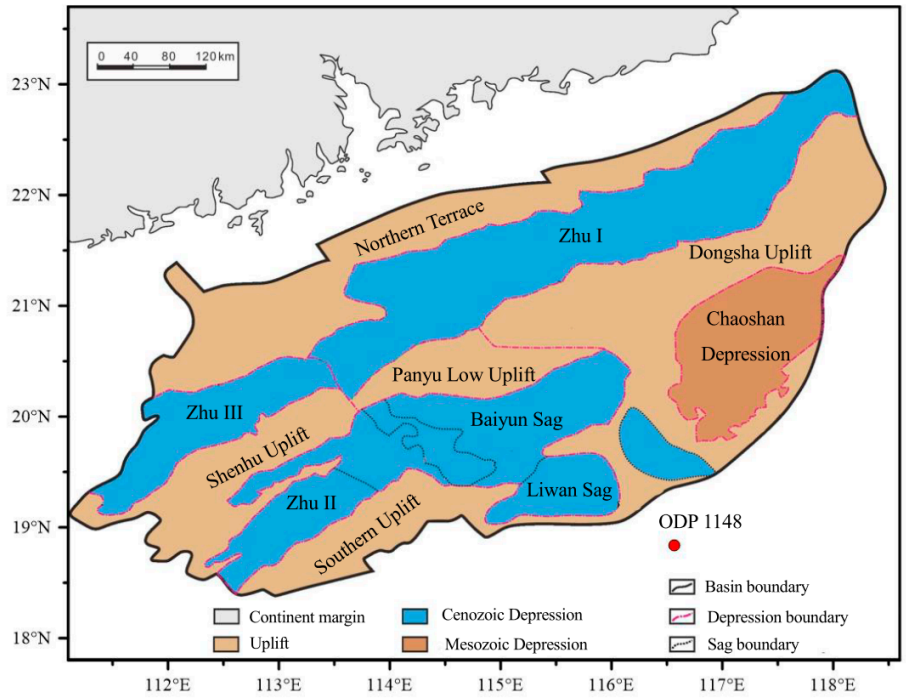

Figure 2. Geological map showing the Pearl River Mouth Basin (PRMB).

Our study suggests that the head scarp of the Baiyun–Liwan submarine slide is located at the northern Baiyun Sag and that the main slide body blankets the Baiyun Sag and the Liwan Sag. The landslide masses moved southeastwards, and some masses were transported to Ocean Drilling Program (ODP) Site 1148 and even further. The landslide extends for over ~250 km, and the total affected area of the slide is up to ~35,000–40,000 km^2.

3. Evidence of the Baiyun–Liwan Submarine Slide

3.1. Shoreward Migration of the Shelf Break

The shoreward shift of the shelf break in the Baiyun Sag provides significant clues about the giant Baiyun–Liwan submarine slide. The present shelf break is aligned with the boundary between the Panyu Low Uplift and the Baiyun Sag, namely the northern Baiyun Sag (Figure 1). The Neogene

sequence stratigraphy of the Baiyun Sag reveals that the shelf break has been located in its present position since ~23.8 Ma, and that the Baiyun Sag was in a deep-water slope environment at that time [26–28]. In Han et al. (2016), detailed results for the evolutionary history of the shelf break showed that the shelf break from 23.8 Ma swung back and forth around the boundary, although it stayed quite close to the present location [22]. However, continental shelf deltaic deposition was found in the Zhuhai Formation (32–23.8 Ma) and was characterized by southward progradational reflections with sigmoid-oblique configurations, while deep-water slope depositional systems from 23.8 Ma were observed [26,29]. In addition, the shelf deltaic deposition extended to the southern Baiyun Sag, and deepwater fan facies were recognized there [22,30]. However, there was a progressive seaward migration from 30 Ma to 23.8 Ma when the shelf breaks were approximately situated in the southern Baiyun Sag. The shelf break migration from the early Oligocene period to the present shows a giant sudden shoreward shift from south to north of the Baiyun Sag at ~23.8 Ma (Figure 3).

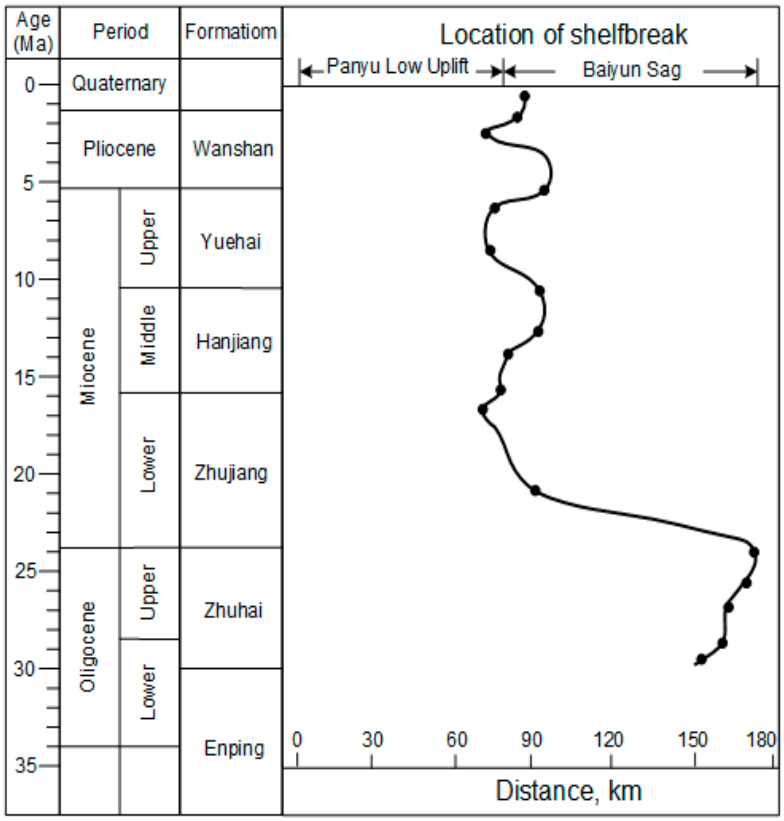

Figure 3. Schematic diagram showing the sequence-stratigraphic framework of the Baiyun Sag and the migration of shelf breaks from 30 Ma to the present in the PRMB. The location of the shelf break was acquired from Han et al. (2016) [22].

The mechanism for shelf break migration is ascribed to sea level changes, sedimentary processes, and geological processes [31,32]. The progressive seaward migration in the southern Baiyun Sag during 30 Ma to 23.8 Ma was proven to be mainly controlled by sediment supply and sea level [22,33]. We attributed the giant sudden shoreward shift from the south to north of the Baiyun Sag ~23.8 Ma ago to a prodigious submarine landslide, namely the Baiyun–Liwan submarine slide. Before the landslide, the Baiyun Sag was part of the continental shelf and in a neritic depositional environment. Therefore, the shelf break was in the south of the Baiyun Sag. After the landslide, a large volume of material was moved from the Baiyun Sag and Liwan Sag to deep water. As a direct consequence, the Baiyun Sag changed from a neritic depositional environment to a deep-water depositional environment, and the shelf break migrated from south to north of the Baiyun Sag.

3.2. Slump Deposition to the Southeast

Slump deposition, found in ODP Core 1148 at ~458–472 mcd (meter composite depth), provides another important piece of evidence for the Baiyun–Liwan submarine slide. ODP Site 1148 (18°50.17′N, 116°33.94′E; water depth 3294 m) is located on the lower continental slope to the southeast of the Baiyun Sag. There, an ~860 m long composite section spanning more than the last 32 Ma was recovered. It was the most offshore site, with the longest core drilled during ODP Leg 184. The dominant lithology at ODP Site 1148 is clay with a variable proportion of nannofossils [34]. The sediment sequence is mainly characterized by three sections: a rapidly deposited Oligocene section (Section 1) and a relatively slowly deposited Miocene to Pleistocene section (Section 3), divided by slumped and faulted intervals at 458–472 mcd (Section 2) [35,36]. Section 2, though similar in composition to the overlying and underlying sections, is dominated by episodic gravitational redeposition, including mass flows and slumping. The Oligocene–Miocene boundary sediments represent massive convolute bedding, soft-sediment plastic deformation, and light-colored carbonate mud clasts of nannofossil chalk, especially at 458–460 mcd (Figure 4). Normal microfaults are common at 460–472 mcd (Figure 4).

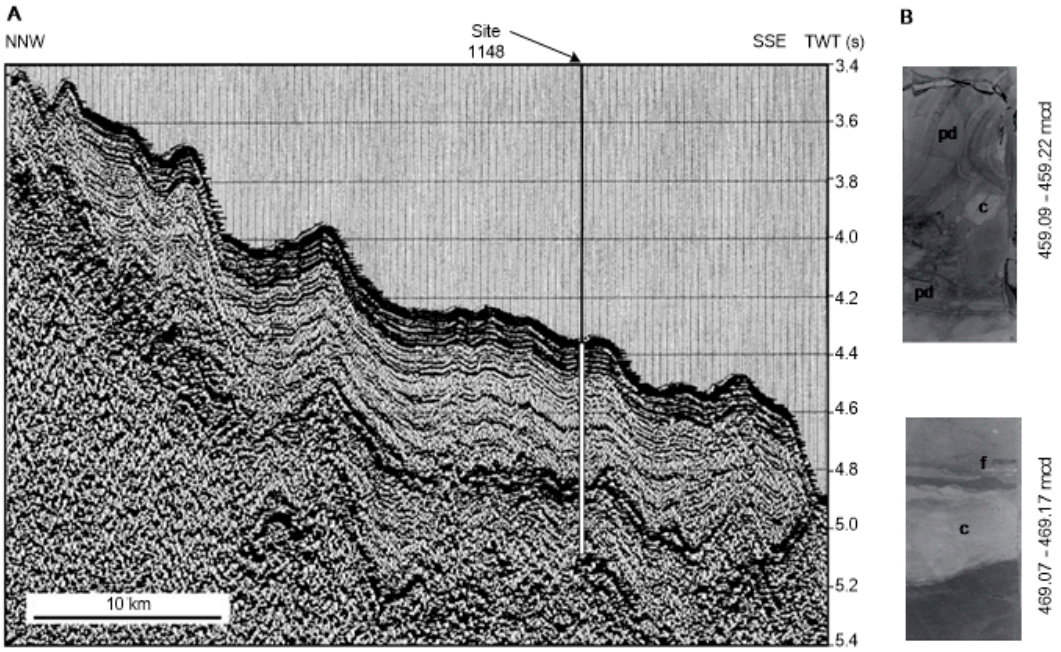

Figure 4. (**A**) Seismic profile through ODP Site 1148, showing a prominent reflector at Section 2, ~5.0 two-way travel time (TWT). (**B**) Section 2 is characterized by plastic deformation (pd), displaced chalk (c), and microfaults (f). Data from Wang et al. (2000) [34].

Coincidentally, the slump deposition is constrained between 23.5 and 24.5 Ma [37]; this epoch is quite close to 23.8 Ma, when the shelf break in the Baiyun Sag shifted from south to north. Given the concurrent events (shift of the shelf break in the Baiyun Sag and the slump deposition at the ODP Site 1148) and the relative elevation (high in the Baiyun Sag and low in ODP Site 1148), we conclude that the Baiyun–Liwan submarine slide does exist and occurred in the Oligocene–Miocene boundary. When the slide occurred, the submarine blocks were removed and transported to the deeper water. Some of these blocks were deposited at ODP Site 1148, forming the slump deposition at 458–472 mcd.

3.3. Decrease in Accumulation Rate

Another noteworthy piece of sedimentary evidence in ODP Core 1148 is the abrupt decrease in the accumulation rate at ~23–24 Ma. The average mass accumulation rates (MAR) decreased from ~7–20 g/cm^2/ky in the early Oligocene to ~1–3 g/cm^2/ky in the Miocene (Figure 5). The distance from the sediment sources may be responsible for the accumulation rates at this location. The higher

accumulation rates of the Oligocene sediments imply active downslope sediment transport from the continental shelf and upper continental slope. After the Baiyun–Liwan submarine slide, the shelf break moved shoreward, far away from the site. Consequently, the greater distance from the sediment sources led to lower accumulation rates at this site, at least within the Neogene. The lower accumulation rates are representative of hemipelagic or pelagic sedimentation.

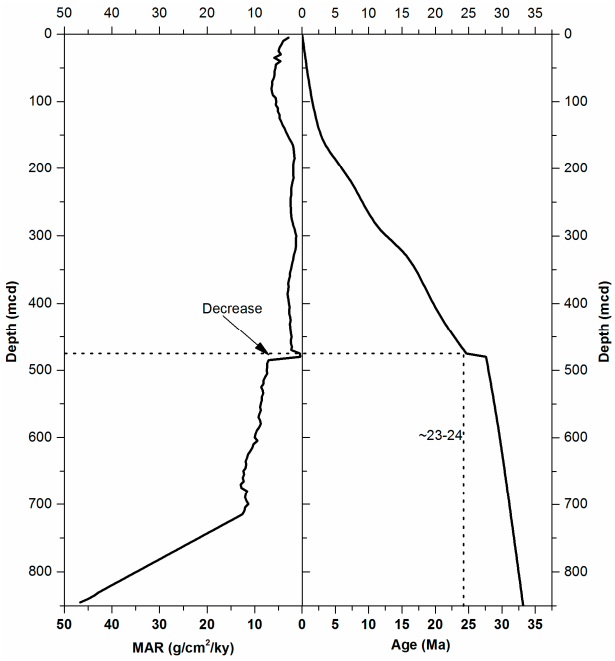

Figure 5. The mass accumulation rates (MAR) vs. depth and the age-depth model for ODP Site 1148. Data from Wang et al. (2000) [34].

4. Discussion

Although many triggering mechanisms can cause landslides, either solely or concurrently, prodigious landslides are more likely to be trigged by tectonic events and global change [6,38–41]. The Storegga slide is attributed to earthquake activity-associated gas hydrate dissociation during postglacial isostatic rebound [42,43]. Volcanic growth is another tectonic activity that causes gigantic landslides both in subaerial environments (e.g., the Markagunt gravity slide—the largest subaerial landslide) [44] and in submarine environments [45].

The Baiyun–Liwan submarine slide seemed to be triggered by other tectonic events e.g., strike–slip movement along the Red River Fault and the ridge jump of the South China Sea. The strain observed by Tapponnier et al. [46] reveals that the penetration of India into Asia extrudes Indochina by more than 500 km southeastwards relative to South China (Figure 6). This strike–slip movement along the Red River Fault occurs at ~22 to 24 Ma at the Oligocene–Miocene boundary. In response to the strike–slip movement along the Red River Fault, the ridge of the South China Sea jumped to the south and changed orientation from nearly E–W to NE–SW at ~24 Ma, which opened the South China Sea [47]. The ridge orientation is exactly perpendicular to the direction of mass movement of the Baiyun–Liwan submarine slide. Our research suggests that the strike–slip movement along the Red River Fault and the ridge jump of the South China Sea contributed to the giant Baiyun–Liwan submarine slide. A steep rise of the Himalayan orogen in the Oligocene–Miocene boundary [48] provides another circumstantial piece of evidence for a triggering mechanism. These coeval events suggest active tectonic activity in the South China Sea and its vicinity in the Oligocene–Miocene boundary. Interestingly, the reversion of strike–slip along the Red River Fault (~5.5 Ma) triggered another prodigious submarine landslide with area of about 18,000 km^2 [49]. More supporting evidence is needed to deepen the understanding of the prodigious Baiyun–Liwan submarine slide and its origin.

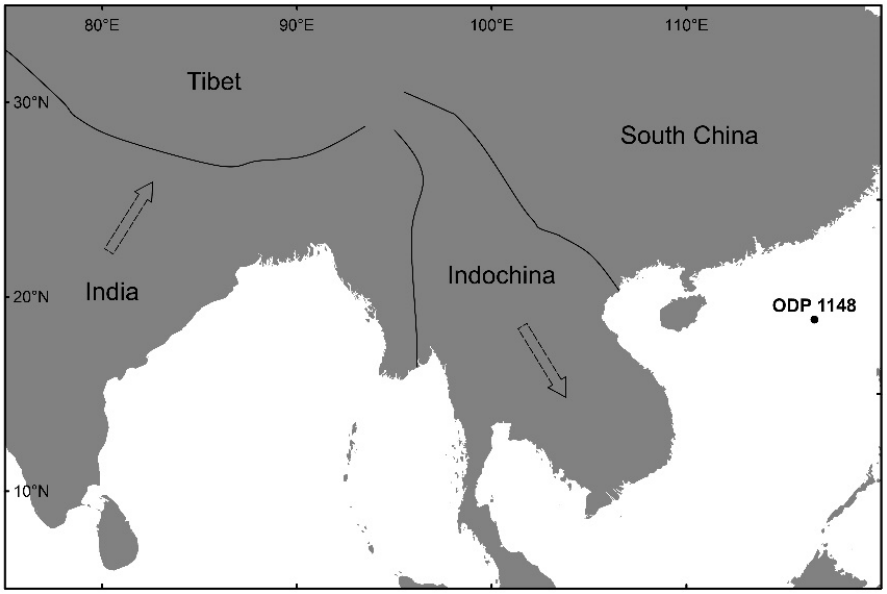

Figure 6. Simplified map showing the triggering mechanism of the Baiyun–Liwan submarine slide.

Given the numerous slope failures subsequent to the Baiyun–Liwan submarine slide in the same place, this area appears to be prone to failure. Nineteen migrating submarine canyons (Figures 1 and 7) have developed on the head scarp of the Baiyun–Liwan submarine slide; and 142 mass transport complexes, each with an average area of over 7 km^2, can be found in the canyons [16,50]. Furthermore, the giant Baiyun slide and the active Dongsha creep, as mentioned in the introduction, are recognized in the affected area of the Baiyun–Liwan submarine slide. Repeated submarine landslides have also been found in other places such as the Gela Basin [51], the Gioia Basin [52], the Eivissa Channel [53], and the Yellow River subaqueous delta [54]. Given the main reservoir of oil, gas, and gas hydrate in the northern South China Sea, more attention needs to be paid to areas of repeated submarine landslides, especially those with many offshore installations.

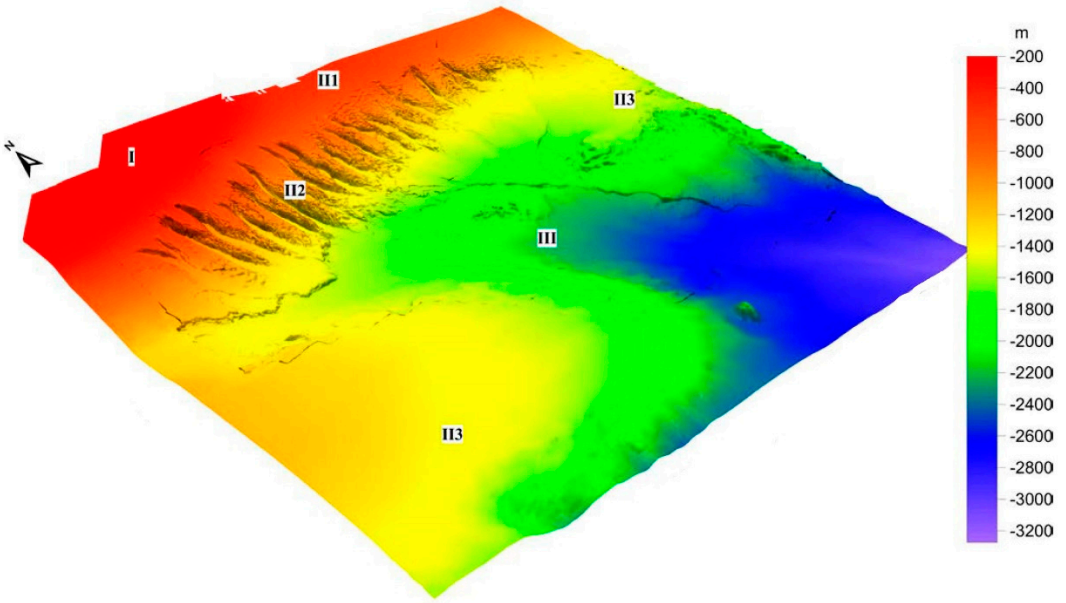

Figure 7. Multi-beam submarine geomorphology shadow map showing the head scarp of the Baiyun–Liwan submarine slide, where the migrating submarine canyons and the Baiyun slide developed on the head scarp of the Baiyun–Liwan submarine slide. I = continental shelf; II1 = upper continental slope; II2 = submarine canyons; II3 = lower continental slope; III = Baiyun slide.

5. Conclusions

Three concurrent events (the shoreward shift of the shelf break in the Baiyun Sag, the slump deposition, and the abrupt decrease in the accumulation rate on the lower continental slope) indicate the giant Baiyun–Liwan submarine slide in the PRMB, South China Sea, at ~23 to 24 Ma, in the Oligocene–Miocene boundary. This landslide extends for over ~250 km, with the total affected area of the slide up to ~35,000 to 40,000 km^2. The scale of the Baiyun–Liwan submarine slide is similar to that of the Storegga slide, which has long been considered to be the largest submarine slide on earth. Our research suggests that coeval events (the strike–slip movement along the Red River Fault and the ridge jump of the South China Sea) in the Oligocene–Miocene boundary triggered the Baiyun–Liwan submarine slide. Attention needs to be paid to areas with repeated submarine landslides and offshore installations.

Author Contributions: Authorship must be limited to those who have contributed substantially to the work reported. Conceptualization, C.Z. and Y.J.; Data curation, C.Z. and Q.L.; Formal analysis, C.Z., S.C. and H.S.; Funding acquisition, Y.J.; Project administration, Y.J.; Visualization, Z.S.; Writing – original draft, C.Z.; Writing – review & editing, S.C., H.S., J.L., X.L. and Y.J.

Funding: This research was funded by the National Natural Science Foundation of China, grant number 41831280 and 41427803, National Key R&D Program of China, grant number SQ2018YFC030044.

Acknowledgments: Authors are indebted to the Ocean Drilling Program Leg 184.

Conflicts of Interest: The authors declare no conflict of interest.

References

1. Korup, O.; Clague, J.J.; Hermanns, R.L.; Hewitt, K.; Strom, A.L.; Weidinger, J.T. Giant landslides, topography, and erosion. *Earth Planet. Sci. Lett.* **2007**, *261*, 578–589. [CrossRef]
2. Korup, O. Earth's portfolio of extreme sediment transport events. *Earth Sci. Rev.* **2012**, *112*, 115–125. [CrossRef]
3. Jia, Y.; Zhu, C.; Liu, L.; Wang, D. Marine Geohazards: Review and Future Perspective. *Acta Geol. Sin. Engl. Ed* **2016**, *90*, 1455–1470. [CrossRef]
4. Talling, P.J.; Clare, M.; Urlaub, M.; Pope, E.; Hunt, J.E.; Watt, S. Large Submarine Landslides on Continental Slopes Geohazards, Methane Release, and Climate Change. *Oceanography* **2014**, *27*, 32–45. [CrossRef]
5. Obelcz, J.; Xu, K.; Georgiou, I.Y.; Maloney, J.; Bentley, S.J.; Miner, M.D. Sub-decadal submarine landslides are important drivers of deltaic sediment flux: Insights from the Mississippi River Delta Front. *Geology* **2017**, *45*, 703–706. [CrossRef]
6. Talling, P.J. On the triggers, resulting flow types and frequencies of subaqueous sediment density flows in different settings. *Mar. Geol.* **2014**, *352*, 155–182. [CrossRef]
7. Soutter, E.L.; Kane, I.A.; Huuse, M. Giant submarine landslide triggered by Paleocene mantle plume activity in the North Atlantic. *Geology* **2018**, *46*, 511–514. [CrossRef]
8. Strasser, M.; Koelling, M.; Ferreira, C.D.S.; Fink, H.G.; Fujiwara, T.; Henkel, S.; Ikehara, K.; Kanamatsu, T.; Kawamura, K.; Kodaira, S.; et al. A slump in the trench: Tracking the impact of the 2011 Tohoku-Oki earthquake. *Geology* **2013**, *41*, 935–938. [CrossRef]
9. Lo Iacono, C.; Gracia, E.; Zaniboni, F.; Pagnoni, G.; Tinti, S.; Bartolome, R.; Masson, D.G.; Wynn, R.B.; Lourenco, N.; de Abreu, M.P.; et al. Large, deepwater slope failures: Implications for landslide-generated tsunamis. *Geology* **2012**, *40*, 931–934. [CrossRef]
10. Zhu, C. Did a submarine landslide worsen the 2018 Indonesia tsunami? *Sci. Prog.* **2019**, *102*, 88–90. [CrossRef]
11. Tan, H.; Ruffini, G.; Heller, V.; Chen, S. A Numerical Landslide-Tsunami Hazard Assessment Technique Applied on Hypothetical Scenarios at Es Vedra, Offshore Ibiza. *J. Mar. Sci. Eng.* **2018**, *6*. [CrossRef]
12. Fine, I.V.; Rabinovich, A.B.; Bornhold, B.D.; Thomson, R.E.; Kulikov, E.A. The Grand Banks landslide-generated tsunami of November 18, 1929: Preliminary analysis and numerical modeling. *Mar. Geol.* **2005**, *215*, 45–57. [CrossRef]
13. Tappin, D.R.; Watts, P.; Grilli, S.T. The Papua New Guinea tsunami of 17 July 1998: Anatomy of a catastrophic event. *Nat. Hazards Earth Syst.* **2008**, *8*, 243–266. [CrossRef]

14. Tappin, D.R.; Grilli, S.T.; Harris, J.C.; Geller, R.J.; Masterlark, T.; Kirby, J.T.; Shi, F.; Ma, G.; Thingbaijam, K.K.S.; Mai, P.M. Did a submarine landslide contribute to the 2011 Tohoku tsunami? *Mar. Geol.* **2014**, *357*, 344–361. [CrossRef]
15. Ding, W.; Li, J.; Li, J.; Fang, Y.; Tang, Y. Morphotectonics and evolutionary controls on the Pearl River Canyon system, South China Sea. *Mar. Geophys. Res.* **2013**, *34*, 221–238. [CrossRef]
16. Chen, D.; Wang, X.; Völker, D.; Wu, S.; Wang, L.; Li, W.; Li, Q.; Zhu, Z.; Li, C.; Qin, Z.; et al. Three dimensional seismic studies of deep-water hazard-related features on the northern slope of South China Sea. *Mar. Pet. Geol.* **2016**, *77*, 1125–1139. [CrossRef]
17. Sun, Q.; Cartwright, J.; Xie, X.; Lu, X.; Yuan, S.; Chen, C. Reconstruction of repeated Quaternary slope failures in the northern South China Sea. *Mar. Geol.* **2018**, *401*, 17–35. [CrossRef]
18. Li, W.; Wu, S.; Voelker, D.; Zhao, F.; Mi, L.; Kopf, A. Morphology, seismic characterization and sediment dynamics of the Baiyun Slide Complex on the northern South China Sea margin. *J. Geol. Soc.* **2014**, *171*, 865–877. [CrossRef]
19. Wang, W.; Wang, D.; Wu, S.; Völker, D.; Zeng, H.; Cai, G.; Li, Q. Submarine landslides on the north continental slope of the South China Sea. *J. Ocean Univ. China* **2018**, *17*, 83–100. [CrossRef]
20. Li, W.; Alves, T.M.; Wu, S.; Rebesco, M.; Zhao, F.; Mi, L.; Ma, B. A giant, submarine creep zone as a precursor of large-scale slope instability offshore the Dongsha Islands (South China Sea). *Earth Planet. Sci. Lett.* **2016**, *451*, 272–284. [CrossRef]
21. Zhang, Y.F.; Sun, Z. A study of faulting patterns in the Pearl River Mouth Basin through analogue modeling. *Mar. Geophys. Res.* **2013**, *33*, 209–219. [CrossRef]
22. Han, J.; Xu, G.; Li, Y.; Zhuo, H. Evolutionary history and controlling factors of the shelf breaks in the Pearl River Mouth Basin, northern South China Sea. *Mar. Pet. Geol.* **2016**, *77*, 179–189. [CrossRef]
23. Zhou, W.; Gao, X.; Wang, Y.; Zhuo, H.; Zhu, W.; Xu, Q.; Wang, Y. Seismic geomorphology and lithology of the early Miocene Pearl River Deepwater Fan System in the Pearl River Mouth Basin, northern South China Sea. *Mar. Pet. Geol.* **2015**, *68*, 449–469. [CrossRef]
24. Xie, H.; Zhou, D.; Li, Y.; Pang, X.; Li, P.; Chen, G.; Li, F.; Cao, J. Cenozoic tectonic subsidence in deepwater sags in the Pearl River Mouth Basin, northern South China Sea. *Tectonophysics* **2014**, *615–616*, 182–198. [CrossRef]
25. Li, J.; Ye, J.; Qin, X.; Qiu, H.; Wu, N.; Lu, H.; Xie, W.; Lu, J.; Peng, F.; Xu, Z.; et al. The first offshore natural gas hydrate production test in South China Sea. *China Geol.* **2018**, *1*, 5–16. [CrossRef]
26. Xu, S.H.; Wang, Y.M.; Xu, G.Q.; Zeng, G.D.; Guo, W.; Gong, C.L.; Cai, C.E.; Tang, W.; Zhuo, H.T.; Wan, H.Q. Linking shelf delta to deep-marine deposition in reservoir dispersal of the upper Oligocene strata in the Baiyun Sag, the northern South China Sea. *Aust. J. Earth Sci.* **2015**, *32*, 365–382. [CrossRef]
27. Pang, X.; Yang, S.; Zhu, M.; Li, J. Deep-water Fan Systems and Petroleum Resources on the Northern Slope of the South China Sea. *Acta Geol. Sin. Engl.* **2004**, *78*, 626–631. [CrossRef]
28. Peng, D.; Chen, C.; Pang, X.; Zhu, M.; Yang, F. Discovery of deep-water fan system in South China Sea. *Acta Pet. Sin.* **2004**, *25*, 17–23.
29. Xie, H.; Zhou, D.; Pang, X.; Li, Y.; Wu, X.; Qiu, N.; Li, P.; Chen, G. Cenozoic sedimentary evolution of deepwater sags in the Pearl River Mouth Basin, northern South China Sea. *Mar. Geophys. Res.* **2013**, *34*, 159–173. [CrossRef]
30. Pang, X.; Chen, C.; Zhu, M.; He, M.; Shen, J.; Lian, S.; Wu, X.; Shao, L. Baiyun movement: A significant tectonic event on Oligocene/Miocene boundary in the northern South China Sea and its regional implications. *J. Earth Sci. China* **2009**, *20*, 49–56. [CrossRef]
31. Fort, X.; Brun, J. Kinematics of regional salt flow in the northern Gulf of Mexico. *Geol. Soc. Lond. Spec. Publ.* **2012**, *363*, 265–287. [CrossRef]
32. Winker, C.D.; Edwards, M.B. Unstable progradational clastic shelf margins. In *The Shelfbreak: Critical Interface on Continental Margins*; Stanley, D.J., Moore, G.T., Eds.; SEPM Society for Sedimentary Geology: Tulsa, OK, USA, 1983; pp. 139–157.
33. Liu, B.; Pang, X.; Yan, C.; Liu, J.; Lian, S.; He, M.; Shen, J. Evolution of the Oligocene-Miocene shelf slope-break zone in the Baiyun deep-water area of the Pearl River Mouth Basin and its significance in oil-gas exploration. *Acta Pet. Sin.* **2011**, *32*, 234–242.
34. Wang, P.; Prell, W.L.; Blum, P. *Proceedings of the Ocean Drilling Program, Initial Reports*; Ocean Drilling Program: College Station, TX, USA, 2000.

35. Li, Q.; Wang, P.; Zhao, Q.; Shao, L.; Zhong, G.; Tian, J.; Cheng, X.; Jian, Z.; Su, X. A 33 Ma lithostratigraphic record of tectonic and paleoceanographic evolution of the South China Sea. *Mar. Geol.* **2006**, *230*, 217–235. [CrossRef]
36. Shao, L.; Pang, X.; Chen, C.; Shi, H.; Li, Q.; Qiao, P. Terminal Oligocene sedimentary environments and abrupt provenance change event in the northern South China Sea. *Geol. China* **2007**, *34*, 1022–1031.
37. Li, Q.; Jian, Z.; Su, X. Late Oligocene rapid transformations in the South China Sea. *Mar. Micropaleontol.* **2005**, *54*, 5–25. [CrossRef]
38. Brothers, D.S.; Luttrell, K.M.; Chaytor, J.D. Sea-level–induced seismicity and submarine landslide occurrence. *Geology* **2013**, *41*, 979. [CrossRef]
39. Zhu, C.; Jia, Y.; Liu, X.; Zhang, H.; Wen, M.; Huang, M.; Shan, H. Classification and genetic machanism of submarine landslide: A review. *Mar. Geol. Quat. Geol.* **2015**, *35*, 153–163. [CrossRef]
40. Chadwick, W.W.; Dziak, R.P.; Haxel, J.H.; Embley, R.W.; Matsumoto, H. Submarine landslide triggered by volcanic eruption recorded by in situ hydrophone. *Geology* **2012**, *40*, 51–54. [CrossRef]
41. Hoffman, P.F.; Hartz, E.H. Large, coherent, submarine landslide associated with Pan-African foreland flexure. *Geology* **1999**, *27*, 687–690. [CrossRef]
42. Canals, M.; Lastras, G.; Urgeles, R.; Casamor, J.L.; Mienert, J.; Cattaneo, A.; De Batist, M.; Haflidason, H.; Imbo, Y.; Laberg, J.S.; et al. Slope failure dynamics and impacts from seafloor and shallow sub-seafloor geophysical data: Case studies from the COSTA project. *Mar. Geol.* **2004**, *213*, 9–72. [CrossRef]
43. Baeten, N.J.; Laberg, J.S.; Vanneste, M.; Forsberg, C.F.; Kvalstad, T.J.; Forwick, M.; Vorren, T.O.; Haflidason, H. Origin of shallow submarine mass movements and their glide planes-Sedimentological and geotechnical analyses from the continental slope off northern Norway. *J. Geophys. Res. Earth* **2014**, *119*, 2335–2360. [CrossRef]
44. Hacker, D.B.; Biek, R.F.; Rowley, P.D. Catastrophic emplacement of the gigantic Markagunt gravity slide, southwest Utah (USA): Implications for hazards associated with sector collapse of volcanic fields. *Geology* **2014**, *42*, 943–946. [CrossRef]
45. Hunt, J.E.; Jarvis, I. Prodigious submarine landslides during the inception and early growth of volcanic islands. *Nat. Commun.* **2017**, *8*, 2061. [CrossRef]
46. Tapponnier, P.; Zhiqin, X.; Roger, F.; Meyer, B.; Arnaud, N.; Wittlinger, G.; Jingsui, Y. Oblique stepwise rise and growth of the Tibet plateau. *Science* **2001**, *294*, 1671–1677. [CrossRef]
47. Briais, A.; Patriat, P.; Tapponnier, P. Updated interpretation of magnetic anomalies and seafloor spreading stages in the south China Sea: Implications for the Tertiary tectonics of Southeast Asia. *J. Geophys. Res. Solid Earth* **1993**, *98*, 6299–6328. [CrossRef]
48. Ding, L.; Spicer, R.A.; Yang, J.; Xu, Q.; Cai, Q.; Li, S.; Lai, Q.; Wang, H.; Spicer, T.E.V.; Yue, Y.; et al. Quantifying the rise of the Himalaya orogen and implications for the South Asian monsoon. *Geology* **2017**, *45*, 215–218. [CrossRef]
49. Wang, D.; Wu, S.; Li, C.; Yao, G. Evidence for submarine landslide in Late Miocene during reversion of strike-slip along the Red River Fault. *Sci. Sin. Terrae* **2016**, *46*, 1349–1357.
50. Zhu, M.; Graham, S.; Pang, X.; McHargue, T. Characteristics of migrating submarine canyons from the middle Miocene to present: Implications for paleoceanographic circulation, northern South China Sea. *Mar. Pet. Geol.* **2010**, *27*, 307–319. [CrossRef]
51. Minisini, D.; Trincardi, F.; Asioli, A.; Canu, M.; Foglini, F. Morphologic variability of exposed mass-transport deposits on the eastern slope of Gela Basin (Sicily channel). *Basin Res.* **2007**, *19*, 217–240. [CrossRef]
52. Gamberi, F.; Rovere, M.; Marani, M. Mass-transport complex evolution in a tectonically active margin (Gioia Basin, Southeastern Tyrrhenian Sea). *Mar. Geol.* **2011**, *279*, 98–110. [CrossRef]
53. Berndt, C.; Costa, S.; Canals, M.; Camerlenghi, A.; de Mol, B.; Saunders, M. Repeated slope failure linked to fluid migration: The Ana submarine landslide complex, Eivissa Channel, Western Mediterranean Sea. *Earth Planet. Sci. Lett.* **2012**, *319–320*, 65–74. [CrossRef]
54. Prior, D.B.; Suhayda, J.N.; Lu, N.Z.; Bornhold, B.D. Storm wave reactivation of a submarine landslide. *Nature* **1989**, *341*, 47–50. [CrossRef]